RSC Advances

ROYAL SOCIETY OF CHEMISTRY

www.rsc.org/advances

Induction of self-structure in polyriboadenylic acid by the benzophenanthridine plant alkaloid chelerythrine: A spectroscopic approach

Ankur Bikash Pradhan[$], Lucy Haque[$], Sutanwi Bhuiya and Suman Das*

Department of Chemistry

Jadavpur University

Raja S. C. Mullick Road, Jadavpur

Kolkata 700 032

India

* To whom all correspondence should be addressed.

Tel.: +91 94 3437 3164, +91033 2457 2349

Fax: +91 33 2414 6266

E-mail:

SD: sumandas10@yahoo.com

ABP: ankurpradhan727@gmail.com

LH: lucy.haque@gmail.com

SB: s.bhuiya12@gmail.com

[$]These authors contributed equally to this work.

Abstract

The naturally occurring benzophenanthridine plant alkaloid chelerythrine (CHL) was found to bind strongly to single stranded polyriboadenylic acid (poly-A) with high association constant of the order of 10^7 M^{-1}. The association was monitored by various spectroscopic and viscometric techniques. Binding of the alkaloid induced self-structure formation of the poly-A helix that showed cooperative melting transition in circular dichroism. Mode of binding of CHL to poly-A was intercalation as revealed from fluorescence quenching, sensitization of fluorescence experiment and viscosity measurement. Transfer of fluorescence energy from RNA bases to CHL has been demonstrated from fluorimetric studies. Thermodynamic data obtained from temperature dependence of binding constant revealed that association was driven by negative enthalpy change and opposed by negative entropy change. Since the interaction of naturally occurring small molecules with RNA is an active area of research, this study renders the scope of exploring chelerythrine as RNA targeted therapeutic agent.

Keywords

Benzophenanthridine alkaloid, single stranded poly-A, Intercalation, Self-structure formation, Fluorescence energy transfer, Thermodynamics.

Introduction

Interactions of small molecules with DNA have been in the focus of exploration since long period in hope to discover effective therapeutic agents. Comparatively less attention has been paid to the study of interaction of small molecules with RNA, which in fact represents a large wealth of targets for the development of novel compounds with pharmacological properties. Study of RNA structures has drawn immense interest to researchers due to the emerging knowledge of their potential and critical roles in many cellular activities.[1,2] The ever growing realization of the variety of biochemical roles of RNA in all living organisms is leading to an increasing appreciation that RNAs provide fascinating targets to treat many infectious diseases. Furthermore, RNA is the genetic material of pathogenic viruses such as HIV or hepatitis C virus (HCV) and thus it provides numerous opportunities for the discovery of new drugs to treat the devastating illnesses caused by these agents.[3-6] However, the identification of RNA-binding drugs is still in its infancy. Therefore interaction studies with various RNA structures with biologically active small molecules are indispensable to understand the basic fundamentals of RNA-ligand interaction.

Most cellular RNA molecules are single stranded, but they may form secondary structures such as hairpin, stem-loop etc. Though there have been many studies that addressed the interactions of small molecules with nucleic acids, comparatively little is known about ligand recognition of single-stranded A-rich RNAs. Among the single stranded nucleic acids, polyriboadenylic acid [hereafter poly-A] is of particular biological significance due to its role in mRNA functioning and gene expression.[7,8] All eukaryotic mRNAs have the long poly-A tail at the 3′ end and it is an important factor for the maturation and stability of mRNA and in the initiation of translation.[9-11] Since the discovery that Neo-PAP (a recently identified human poly-A polymerase) is significantly

over expressed in some human cancer cells, it has been suggested that the poly-A tails of mRNA might interfere with the full processing of mRNA by PAP and switch off protein synthesis.[12-14] This suggests that poly-A tail is a potential tumor-specific target.[14] The control of such over expression of poly-A by the binding of small molecule drugs could be a potential means to RNA targeted therapeutic intervention. Poly-A has the unique characteristics to exist in single stranded helical and parallel double stranded structure in *vitro*.[15-17] The structure of the double helix has been established from X-ray crystal analysis.[15] Recently, it has been shown that a variety of small molecules bind to single stranded poly-A and induce unique structural transformation to a self-structure stabilized by adenine–adenine base pairs.[18-24] *In vivo*, such molecules which can bind and structurally modulate the polyadenylate tail could stop poly-A chain elongation, inhibit mRNA function and stop subsequent protein production in the cell.

Naturally occurring small molecules have been in the center of attention as therapeutic agents for their high abundance and low side effects. The alkaloids represent a very extensive group of nitrogen-containing secondary metabolites with diverse structures, distribution in nature and important biological activities. The biological activity of alkaloids has been known to play important roles in medicinal chemistry due to their interaction with nucleic acids. The study of interaction mechanism between many alkaloid molecules and DNA/RNA has encouraged the development of new drugs.[25-26] Among the alkaloids, benzophenanthridine group of plant alkaloids have been the focus of increasing attention for its wide range of biological activities.[27-34] Compounds of this group exhibit strong nucleic acid binding ability as well as inhibitory effects of different important enzymes.[35] One of the remarkable structural features of the benzophenanthridine alkaloid is their ability to show pH dependent structural transition between the iminium and alkanolamine forms.[36] Among the benzophenanthridine group of alkaloids, sanguinarine is

a well studied compound. It shows diverse biological activity as well as strong nucleic acid binding capacity.[21] Sanguinarine has been reported to interact with different polymorphic forms of nucleic acid structures.[37] It induces self structure to poly-A under specific environmental condition and also binds to the double stranded form of poly-A.[21,38] Chelerythrine (hereafter CHL, Fig. 1) (1,2-dimethoxy-12methyl[1,3]benzodioxolo[5,6-*c*]phenanthridin-12-ium) is another benzophenanthridine alkaloid, which slightly differ from sanguinarine in the type and position of substituents in the structure. CHL exhibits pronounced cytotoxicity,[31,39] anticancer[28,34] and antitumour activity.[29,34] CHL is a potent protein kinase C inhibitor and also inhibits the anti-apoptotic Bcl-2 family proteins.[40] This compound has been shown to initiate the rapid mitochondrial apoptotic death of H9c2 cardiomyoblastoma cells.[40] CHL shows significant anti-proliferative activities suggesting that it can be considered as agent promising for cancer therapy.[41] CHL has been reported to activate p38 MAP kinase and JUNK signaling pathways and induce apoptosis in cancer cells both *in vitro* and *in vivo*.[34,39,42,43] Recent studies have revealed that CHL can exist between iminium form (charged) and alkanolamine form (uncharged) with a pK_a of 8.58.[44] There are few studies on the DNA binding of CHL.[33,45] Very recently a detail study on the interaction of this compound with DNA has been reported by Basu *et al*.[44] They have reported that the iminium form of CHL binds to DNA by intercalation, while the alkanolamine form does not bind at all to DNA. However, their studies are limited to calf thymus (CT) DNA and no work has been reported so far by any other group on the interaction of CHL with RNA. Keeping in view of the diverse biological effects of CHL and importance of structure and function of poly-A, our focus is to study the interaction of CHL with poly-A using different spectroscopic and viscometric techniques. Overall, our aim is to elucidate and understand the structural and energetic aspects of CHL binding to poly-A and its capability to induce self structure formation to single stranded poly-A.

Experimental Section

Materials

Both CHL and poly-A were purchased from Sigma Aldrich Corporation (St. Louis, MO, USA). They were used without further purification. Concentration of CHL was checked spectrophotometrically by using known molar absorption coefficient value of 37060 M^{-1} cm^{-1} at 316 nm.[44] The solutions of CHL were kept in dark all time to avoid any light induced photochemical change. A molar absorption coefficient value of 10000 $M^{-1}cm^{-1}$ at 257 nm was used to calculate the concentration of poly-A solution.[14] No deviation from Beer's law was observed in the experimental concentration range employed in this study. Fresh solution of CHL was prepared each day for better experimental results. 10 mM citrate phosphate buffer containing 25 mM NaCl of pH 6.5 (CPB buffer) was used for all experiments. Distilled deionized water and analytical grade reagents were used for preparation of the buffers. All buffer solutions were filtered through millipore filters of 0.45 μm pore size before use. Under our buffer condition CHL remained almost cent percent in the iminium form. At the same time free poly-A remained in the single stranded form in the experimental buffer condition containing 25 mM NaCl as evidenced from observed CD spectrum.

Methods

UV-Absorption experiments

All the UV-VIS absorbance studies were made on a Shimadzu model UV-1800 spectrophotometer (Shimadzu Corporation, Japan) in matched quartz cells of 1 cm path length. A thermoprogrammer was attached to it to maintain the temperature of this spectrometer by peltier effect. Initially, to a fixed concentration of CHL small aliquots of poly-A were added to verify whether there were any interaction of CHL with RNA. In this

case maximum aliquot volume was 2 μl and total added volume of poly-A solution was such that the final dilution remained within 1% .

Typical hypochromism and bathochromism of CHL absorption was noted along with the appearance of isosbestic point. This clearly indicated binding equilibrium between the alkaloid and the RNA polymer. But in this process there is a limitation that we cannot reach very high ratio of polymer to the ligand as saturation was reached earlier. To avoid this problem, spectrophotometric titrations were performed using the methodology described previously.[37,46] In this method we could start with a very high value of ratio of polymer to the ligand. Briefly a known concentration of poly-A was kept in the sample and reference cells and small aliquots of a known concentration of CHL were added into the sample cell. After each addition, solution was mixed and allowed to re-equilibrate for at least 5 minutes before recording the data. To avoid possible aggregation and prevent adsorption to the walls of the cuvette, the absorbance values were kept at the minimum for optical studies. This spectrophotometric data were then cast into Scatchard plots of r/C_f versus r as described previously.[37,46]

Spectrofluorimetric studies

Steady state fluorescence measurements were performed on a Shimadzu RF-5301PC spectrofluorimeter (Shimadzu Corporation, Kyoto, Japan) which was attached to a highly sensitive temperature controller. Measurements were made in fluorescence free quartz cell of path length of 1 cm. A fixed concentration of CHL was titrated by increasing concentration of poly-A under constant stirring condition. All the measurements were conducted keeping an excitation and emission band pass of 5 nm.

Analysis of binding data and evaluation of binding parameters.

Spectrophotometric and spectrofluorimetric titration data were used to construct Scatchard plots of r/C_f versus r.[47] In case of spectrophotometric titration we have used the data from

direct titration as well as reverse titration and we have used the direct titration in spectrofluorimetry. The advantage of reverse titration is that we could get data up to very low value of r, whereas we had limitation to reach such low value of r in the direct titration. All the Scatchard plots were nonlinear and showed negative slopes at low r values as observed in non-cooperative binding isotherms and hence were analyzed by excluded site model for non-linear non-cooperative ligand binding phenomenon using McGhee and von Hippel equation,[48]

$$\frac{r}{C_f} = K'(1-nr)\left[\frac{(1-nr)}{\{1-(n-1)r\}}\right]^{(n-1)} \qquad (1)$$

where, K′ is the intrinsic binding constant to an isolated site, n is the number of the nucleotides occluded after the binding of one single ligand molecule, r is the number of moles of CHL bound per mole of nucleotide and C_f represent free CHL concentration. The binding data were analyzed using the Origin 7.0 software to determine the best-fit parameters of K′ and n.

Determination of Binding Stoichiometry

Job's continuation method[49] was employed to find the binding stoichiometry of CHL with poly-A by using the fluorescence spectroscopy. At constant temperature the fluorescence intensity (λ_{max}=564 nm) was measured for the solution where concentration of both poly-A and ligand were varied but the sum of their concentrations kept constant at 10 μM. The relative difference of fluorescence intensity of CHL at 564 nm was plotted against the mole fraction of CHL. The break point of the plot gave the mole fraction of CHL in complex. The stoichiometry was obtained in terms of poly-A:CHL [$(1-\chi_{CHL})/\chi_{CHL}$] where χ_{CHL} denotes the mole fraction of CHL. The results reported are average of at least three experiments.

Fluorescence polarization anisotropy

The steady state fluorescence anisotropy was also measured using the same spectrofluorimeter. Steady state anisotropy (r′) was defined by,[50]

$$r' = \frac{(I_{VV} - G \cdot I_{VH})}{(I_{VV} + 2G.I_{VH})} \qquad (2)$$

where, G is the ratio I_{HV}/I_{HH} used for instrumental correction. I_{VV}, I_{VH}, I_{HV} and I_{HH} represent the fluorescence signal for excitation and emission with the polarizer positions set at (0,0), (0,90), (90,0) and (90,90) respectively. The excitation and emission wavelengths were fixed at 400 nm and 564 nm respectively. The excitation and emission slit width were fixed at 5 nm. Readings were observed 5 min after each addition to ensure stable complex formation. Each reading was an average of five measurements. Anisotropy values were plotted as a function of increasing poly-A concentration.

Mode of binding: fluorescence quenching studies

Fluorescence quenching studies were carried out with the anionic quencher potassium iodide. Solution of KI was mixed with the solution of KCl in different proportions to give a fixed total ionic strength. Quenching experiments were performed at a constant P/D ratio (P/D= nucleotide/CHL molar ratio) monitoring fluorescence intensity changes at 564 nm as a function of concentration of the iodide. The data were plotted in the form of Stern-Volmer equation,[51]

$$\frac{F_o}{F} = 1 + K_{SV}[Q] \qquad (3)$$

Where, F_o and F are the fluorescence intensities of the alkaloid-complex with poly-A (P/D=6 where complete saturation was assured) in the absence and in the presence of the quencher (Q) KI and K_{SV} is the Stern-Volmer quenching constant. K_{SV} is indicative of the accessibility of the bulky quencher (iodide) to the fluorophore CHL. The slope of the F_o/F *versus* [KI] plot yield the value of Ksv.

Viscometric study

Viscometric measurements were carried out using a Cannon-Manning semi micro dilution viscometer type 75 (Cannon Instruments Co., State College, PA, USA) submerged vertically in a constant temperature bath maintained at 25±0.5 °C. The molecular weight of poly-A sample was estimated to be in the order of 2–2.5x10^5 Da with an intrinsic viscosity of 2.7 dL/g. 700 μL of 500 μM RNA solution was placed in the viscometer and aliquots of stock solution of CHL were directly added into the viscometer to obtain increasing D/P (CHL/nucleotide molar ratio) values. After each addition of CHL to the solution of poly-A in the viscometer, mixing was assured by passing air bubble slowly through the solution using narrow teflon tube. Flow times of poly-A in absence and in presence of increasing concentration of CHL were measured after allowing an equilibration time of 15 minutes. Measurements were done in triplicate with an accuracy of ±0.01 s and the relative specific viscosity was calculated using the equation:

$$\frac{\eta'_{sp}}{\eta_{sp}} = \frac{[t_{complex} - t_0]}{[t_{control} - t_0]} \qquad (4)$$

Here, η'_{sp} and η_{sp} are the specific viscosity of poly-A in presence and in absence of CHL; $t_{complex}$ and $t_{control}$ are the time of flow of complex and control solution and t_0 is the same for buffer solution as described previously.[52]

Sensitization of alkaloid emission, quantum efficiency determination and fluorescence energy transfer

Excitation spectrum of CHL was recorded in the wavelength range of 220-310 nm to study the energy transfer from RNA bases to CHL. The excitation spectrum was recorded by monitoring the emission wavelength at 564 nm. This was confirmed further by recording of the nucleobase sensitized emission spectrum of CHL in the wavelength region 500-650 nm.[53] The quantum efficiency (Φ) of a ligand is a measure of amount of energy transfer from nucleic acid to ligand upon binding. Φ was evaluated for different wavelengths from

the ratio of the quantum efficiency of the ligand (CHL) bound to nucleic acid (ϕ_b) to the quantum efficiency of free CHL (ϕ_f) using the equation,[54]

$$\Phi = \frac{\phi_b}{\phi_f} = \frac{I_b}{I_f} \times \frac{\varepsilon_f}{\varepsilon_b} \qquad (5)$$

where, I_b and I_f are the fluorescence intensities of bound and free CHL respectively. These values were obtained during fluorescence titration of CHL by poly-A. ε_f is molar absorption value of free CHL which is already known. Calculation of determining ε_b value has been described by Garbett *et al.*[55] The ratio between the quantum efficiency of bound CHL excitation in the UV spectral region (Φ_λ) to that at 310 nm (Φ_{310}) was calculated. The wavelength 310 nm was chosen for the normalization process because of insignificant absorbance of RNA at this wavelength.

Circular dichorism spectral studies.

Circular dichroism (CD) measurements were carried out on a PC-driven JASCO J815 spectropolarimeter (Jasco International Co., JAPAN) attached with a temperature controller and a thermal programmer model PFD-425L/15 interfaced in a rectangular quartz cuvette of 1 cm path length. All CD spectra were recorded in the wavelength range of 200–450 nm with a scan speed of 100 nm/min. Each spectrum was averaged from five readings. Final CD spectra were expressed in terms of molar ellipticity ([θ]) in units of deg cm^2 $dmol^{-1}$ by using the software provided with the spectropolarimeter. The molar ellipticity is based on poly-A concentration.

Thermal melting studies.

The denaturation profiles of poly-A in the absence and in the presence of CHL were taken in the same spectropolarimeter by monitoring the change in CD at 264 nm. The rate of heating was 0.5 °C min^{-1} in the temperature range of 15 °C to 100 °C.

Thermodynamic studies: temperature dependent spectrophotometry

Temperature dependent absorption spectra were recorded by using Shimadzu UV-1800 double beam spectrophotometer attached with thermometric cell temperature programmer and temperature controller. These measurements were performed at 15, 20, 25 and 35 °C allowing an equilibrium period of 10 minutes for each addition.

Evaluation of thermodynamic parameters

The values of K′ and n were determined at different temperatures using UV-visible spectrophotometric measurements. Thermodynamic parameters were estimated by analysis of van't Hoff plot (ln K′ versus 1/T) obtained over the temperature range of the study. The slope of the plot gives the binding enthalpy change (ΔH^{o}) as

$$\partial \ln\left(K'\right) / \partial\left(1/T\right) = -\frac{\Delta H^{o}}{R} \qquad (6)$$

The Gibbs free energy change (ΔG^{o}) was determined from the binding constant at a particular temperature according to this relation

$$\Delta G^{o} = -RT \ln\left(K'\right) \qquad (7)$$

The entropy change (ΔS^{o}) was then estimated from the following equation

$$\Delta S^{o} = \left(\Delta H^{o} - \Delta G^{o} / T\right) \qquad (8)$$

Results and Discussion

UV-Vis absorption spectral studies

It is known that binding of small molecules with nucleic acid can be monitored by employing absorption spectral titration when the former has absorption characteristics where nucleic acids do not absorb.[44] The absorption spectral study on the interaction of CHL with poly-A in CPB buffer at 25 °C is represented in Fig. 2A. With increase in concentration of RNA the maximum absorption peak (~316 nm) of the alkaloid was red shifted for about 5 nm and at the same time a significant hypochromic effect was noted.

Such finding can be rationalized as follows: the empty π^*-orbital of the ligand molecule couples with the π^*-orbital of the RNA bases causing an energy decrease, and a decrease of the π–π^* transition energy. As a result a bathochromic shift is noted. Again, the empty π^*-orbital is partially filled with electrons to reduce the transition probability, which causes hypochromism.[56] The presence of sharp isosbestic point at 466 nm indicated the presence of two state systems consisting of bound and free alkaloid species enabling application of equilibrium conditions in the complexation. A summary of the optical properties of free and RNA bound form of CHL are given in (Table S1). The data obtained from reverse spectrophotometric titration (described earlier) were cast into the form of Scatchard plot of r/C_f versus r (Fig. 3A). It was found that the plot was nonlinear and there was always negative slope for all r values. Such negative value of slope for whole range of r indicated noncooperative type of binding. In this case it is to be noted that we could not reach very low value of r when we used the direct titration of CHL with increasing amount of poly-A. The plot was fitted and analyzed by non-cooperative binding using McGhee-von Hippel equation.[48] The binding constant was found to be (2.06±0.1) x10^7 M^{-1} and the number of bases occluded (n) for a single CHL molecule was ~2. Till today, such high binding affinity of any naturally occurring small molecule with poly-A has not been reported. So far the maximum binding affinity of a ligand, that includes either DNA intercalator or groove binder, to poly-A has been reported to be around 1x10^7 M^{-1}.[18,21,22,57] Very recently, Kumar and his group reported the detail investigation on the interaction CHL with calf thymus (CT) DNA where binding affinity was in the order of ~ 10^5 M^{-1}.[44]

Fluorescence spectral studies

Binding of CHL with poly-A was further investigated by fluorescence intensity measurements. The emission spectrum of CHL was recorded in the wavelength range 430-800 nm by exciting at 400 nm. The emission maximum was found around 564 nm when

excited at 400 nm. Representative excitation spectra of the iminium and alkanolamine forms of CHL (keeping emission fixed at 564 nm) are shown in Fig. S1.

In the pH range above 10.0, CHL exists almost exclusively in the alkanolamine form and it exists in almost exclusively in the iminium form when the pH of the medium is below 6.7.[44] In our experimental condition pH was maintained at 6.5 which ensured that CHL was exclusively in the iminium form structure. From the absorption spectrum of alkanolamine form it is observed that there is no absorption around 400 nm, while for iminium form of CHL strong absorption band is present around 400 nm. Thus the absorption band around this wavelength is characteristic feature of the iminium form and not the alkanolamine form. Excitation spectrum of alkanolamine form of CHL (keeping emission fixed at 564 nm) shows the absence of any band around 400 nm, while there is a strong band for the iminium form spectrum. From the absorption and excitation spectra of the two forms of CHL it is clear that the emission at 564 nm for CHL was solely from iminium form of the alkaloid when excited at 400 nm (though presence of very trace amount of alkanolamine form at equilibrium cannot be ruled out). In other words, excitation wavelength of 400 nm instead of 316 nm or 350 nm was chosen to ensure the excitation of iminium form of CHL only and not the alkanolamine form. In our study we are only interested with the iminium of form of the alkaloid.

Complex formation was monitored by titration studies keeping a constant concentration of the alkaloid and increasing the concentration of poly-A. With increasing concentration of poly-A a progressive enhancement in the fluorescence intensity of the alkaloid was observed and eventually reaching a saturation point with ~3 nm blue shift in the wavelength maximum (Fig. 2B). The results of the spectrofluorimetric titrations were analyzed by constructing Scatchard plot. The Scatchard plot (Fig. 3B) exhibited non-cooperative behaviour as revealed by negative slope and hence was analyzed further by

the McGheee and von Hippel methodology for non-cooperative binding. Analysis yielded a binding constant of (2.14±0.07) x10^7 M^{-1} and n value of 2.32±0.04 (at 25 ºC). The binding parameters obtained from spectrofluorimetry are in excellent agreement with the spectrophotometric results (Table 1).

Evaluation of binding stoichiometry

The stoichiometry of association of CHL with poly-A was determined independently by continuous variation analysis (Job's plot) in fluorescence spectroscopy. Throughout the experiment total concentration of poly-A and CHL was fixed at 10 μM. The mole fraction of CHL was varied from 0 to 1. The ratio of difference in fluorescence intensity ΔF (difference in fluorescence intensity of CHL in presence and absence of poly-A) and intensity of free CHL (F_o) was plotted against the mole fraction of CHL (Fig. S2). An inflection point was observed at χ_{CHL}=0.34. The stoichiometry of the poly-A-CHL was found to be 2:1 in terms of poly-A:CHL. This value is in good match with the values calculated from spectrophotometric and spectrofluorimetric titrations (Table 1).

Fluorescence polarization anisotropy

Fluorescence anisotropy measurements provide effective information about the nature of the environment of biological probes. Any factor affecting shape, size and flexibility of a molecule affects the observed anisotropy.[51] Increase in the rigidity of the environment surrounding the fluorophore is manifested in an increase in the fluorescence anisotropy. Change in anisotropy can thus helps us in finding the probable location of a probe in micro-heterogeneous environments like proteins, nucleic acids.[58] The variation of fluorescence anisotropy of CHL with increasing concentration of poly-A is shown in Fig. S3. A significant increase in the fluorescence anisotropy on binding with poly-A suggested that the dye was trapped in a motionally restricted region within the polynucleotide. The fluorescence polarization upon binding of CHL to the poly-A showed a value of ~0.13 at

saturation against a value of ~0.04 for free CHL under identical condition. Our result indicates that CHL binds strongly to poly-A structure probably by intercalation between the bases.

Fluorescence quenching study and mode of binding

Fluorescence quenching experiment provide an effective method to address the mode of binding of small ligand to nucleic acids.[51] In principle, molecules that are either free or bound on the surface of nucleic acid are easily accessible for the quencher while those are inserted between the bases of the polynucleotide may be inaccessible from the quencher. Negative charge on the phosphate groups causes an electrostatic barrier at the helix surface and limits the penetration of an anionic quencher into the interior core of the helix. Hence very little or no quenching may be observed in the presence of such quencher if the binding involves strong stacking. As a result the magnitude of the Stern-Volmer quenching constant (K_{SV}) of the ligands that are bound inside will be lower than that of the free molecules. It is known that intercalation of small molecules into the DNA double strands protects the entrapped molecules from an ionic quencher.[59-61] Electrostatic binding and groove binding, on the contrary, leave the probe molecule exposed to the bulk aqueous phase and does not appreciably obstruct the approach of the quencher to it.[59] Compared to intercalative binding groove binding offers much less protection for the fluorophore.[61] It is observed that binding to the poly-A resulted in increase in fluorescence intensity of CHL (Fig. 2B). Representative Stern-Volmer plots for free and RNA bound CHL are shown in Fig. S4. K_{SV} values for free CHL and its complex with poly-A were 12.5 and 6.2 L mol^{-1} respectively. This indicates that the bound CHL is less accessible to the quencher which in turn tells that the bound alkaloid molecules are considerably protected and sequestered away from the solvent. This observation leads us to suggest intercalative mode of binding of CHL with poly-A. Similar observation has been reported

for the binding of CHL to CT DNA.[44] We have done the quenching experiments in solutions of higher ionic strength (in presence of 0.1M NaCl). But the Stern Volmer quenching constant was found to be almost unaffected. This also made confirmed the binding mode to be intercalation and not groove binding.

Viscometric study

To investigate the mode of binding of the alkaloid to poly-A helix viscosity study was undertaken (Fig. 4). The relative specific viscosity of the poly-A-alkaloid complex increased with increase in D/P. Since hydrodynamic measurements are sensitive to length changes, they are regarded as the most critical for elucidating the binding mode of small molecules to nucleic acids in solution.[59] Our results clearly underscore the intercalation type of binding of CHL to poly-A helix. Nevertheless, since single stranded poly-A has only stacked helical structure (no base pairing) a true intercalation model[59] where planar ligand molecules are fully sandwiched between hydrogen-bonded base pairs of double stranded DNA cannot be ideated. This data along with the hypochromism in the absorbance spectrum and fluorescence quenching results support an intercalating complexation of CHL with poly-A.

Energy transfer from RNA bases to bound CHL

Strong interaction between CHL and poly-A was evidenced from spectrophotometric and spectrofluorimetric titration. Fluorescence quenching studies along with viscometric data clearly indicate intercalative binding of the alkaloid to the poly-A helix. The chance of excited energy transfer from the bases of poly-A to the bound CHL molecules (Fig. 5D) was explored by measuring the excitation spectrum of CHL. Fluorescence emission was monitored at 564 nm and the excitation was varied from 220 to 550 nm. Energy transfer was studied by recording the excitation spectrum of CHL in presence of poly-A (in the concentration ratio CHL:poly-A=1:10). In absence of poly-A the observed excitation

spectrum of CHL (curve 1, Fig. S5) matches with that of its absorption spectrum in the wavelength region 300-550 nm (Curve 1, panel A, Fig. S1). But in this case there was almost absence of any band in the excitation spectrum around 260-280 nm, though there was presence of a strong peak around this wavelength in the original alkaloid absorption spectrum (Curve 1, panel A, Fig. S1). This observation indicated that the emission of CHL at 564 nm might not be due to the absorption around 260-280 nm band. This was further confirmed from the emission spectrum of free CHL when it was excited at 270 nm. In this case we did not get any significant emission in the wavelength range 300-600 nm. The absorption of CHL in the region of 220-300 nm is weak compared to that of RNA which shows a strong absorption around 260 nm. In the excitation spectrum of RNA bound CHL we got very high intensity in the wave length region of 220-300 nm (not shown) which was very weak in case of free CHL. In control experiments, pure RNA solutions showed almost no excitation bands in the 220-300 nm region when monitored at 564 nm (curve 2 of Fig. S5). The ratio of excitation spectra of CHL-poly-A complex is presented in Fig. 5A. This plot indicates direct emission from CHL and the ratio greater than unity indicates sensitization by RNA. Appearance of very strong excitation band around 270 nm in the bound complex can only be explained on the basis of absorption of energy and then its transfer by the RNA bases to the alkaloid. Absence of any band in the excitation spectrum of RNA in the wavelength region 220-300 nm, when emission was monitored at 564 nm, is consistent with the interpretation of energy transfer from RNA to CHL. The energy transfer from RNA to the alkaloid was further confirmed from sensitized emission of the complex which is more intense than direct emission of CHL (Fig. 5B). Fluorescence energy transfer from the RNA bases to the bound CHL molecules was manifested in the enhancement of quantum efficiency of bound molecules in the wavelength range of RNA absorption. It has been demonstrated earlier that such type of energy transfer from DNA

base to ligand occurs efficiently when the ligand is intercalated in DNA structure where the DNA bases are in close contact with the ligand.[54] Similar observations have also been reported by Kumar and his group.[62] They have shown that such energy transfer depends on the sequence of nucleic acid polymer. Since energy transfer occurs due to close contact, from such sensitization study, both strong binding as well as intercalative mode of binding of CHL to poly-A is further confirmed. A plot of Φ_λ/Φ_{310} against wavelength at a P/D (RNA base/CHL molar ratio) of 10 is shown in Fig. 5C. An increase in quantum efficiency in the RNA absorption region was observed. This implies energy transfer from the RNA bases to bound alkaloid molecules and also indicates intercalative mode of binding. Reprehensive scheme for energy transfer is shown in the Fig. 5D. Such fluorescence energy transfer has been reported in case of CHL-DNA binding.[44] Thus from our study along with the study of Pritha *et al* it can be concluded that both DNA and RNA bases can transfer energy to CHL when the alkaloid is intercalated in the DNA/RNA structure.

Spectropolarimetric results

CD spectral study on the binding of CHL to poly-A

Conformational changes in poly-A on binding of CHL was investigated from intrinsic circular dichroism studies. The intrinsic CD spectra of poly-A showed a large positive band around 262 nm and a negative band around 245 nm followed by a small positive band around 220 nm. On the other hand, the benzophenanthridine alkaloid, CHL does not have any intrinsic CD activity. To examine the CHL-induced changes in the conformation of poly-A, the CD spectra was recorded in the region of 200-400 nm under varying D/P values. CD spectral changes of poly-A on interaction with CHL are presented in Fig. 6. CD spectra demonstrate that the conformation of poly-A undergoes a remarkable change in presence of CHL. The decrease in intensity of CD bands around 245 and 262 nm implies an alteration of poly-A structure upon addition of CHL. The broad band at 262 nm

disappeared at the saturation whereas an increase of the negative band maximum at ~245 nm was observed till the saturation. Similar kind of observation has been reported for the interaction of coralyne with poly-A.[18] Four clear isoelliptic points at 210, 238, 251 and 320 nm were observed for the poly-A-CHL interaction. The appearance of induced CD band in the region of 290-370 nm clearly indicates the binding of CHL in the asymmetric environment of poly-A helix.

CD melting Study

CD data presented previously clearly suggested the alteration of the poly-A secondary structure in presence of CHL and also a strong asymmetric environment of the bound alkaloid in the helical structure of the polynucleotide. This is presumably due to intercalative binding. Similar kind of observations on the interaction of another benzophenanthridine alkaloid sanguinarine with poly-A have been reported by Giri and Kumar.[21] More often in DNAs, the alteration from A to B-form and from B to C-like forms manifest as large decrease of ellipticity of the long wavelength band. A direct correlation of such alteration of the CD bands with the helix parameters are complex.[63] But an ordered structural transition like the formation of duplex structure can be assumed to occur and this may be assisted by the efficient screening of charges of the phosphate backbone by the intercalated positively charged CHL. Giri and Kumar have shown the self-structure formation of poly-A by the benzophenanthridine alkaloid sanguinarine.[21] Ren and colleagues reported similar self-structure formation in poly-A in presence of coralyne.[18] Prior to that, Hud's laboratory observed the ability of coralyne to disproportionate the duplex poly(dA). poly(dT) into poly(dT). poly(dA).poly(dT) triplex and a coralyne-poly(dA) self-structure.[64] To examine whether the binding of CHL could induce the self-structure formation in poly-A we investigated the melting behaviour of poly-A employing CD melting. The characteristic CD spectra of single stranded poly-A in

absence and in presence of CHL are shown in Fig. 7A. The melting was monitored at 264 nm and the profiles are depicted in Fig. 7B and 7C. We found cooperative melting of poly-A-CHL complex in CD (Fig. 7C), while no such cooperative change was found in case of free poly-A (Fig. 7B). In absence of CHL the slow change in CD is attributed to the helix to coil transition of poly-A.[65] The melting temperature of poly-A-CHL complex was found to be ~ 62 °C. Such cooperative transition in the melting profile of the complex unequivocally confirmed the formation of self-assembly structure. Self-assembled structure induction in poly-A by planar molecules has been supported by intercalative geometry and the melting results confirm such helical organization induced by CHL. Induction of self-structure in poly-A by different DNA intercalators, partial intercalators and groove binders has been reported.[22,57] From the observations of Kumar and his group it appears that compounds bind cooperatively only induce self-structure formation in poly-A. This is found to be true for many small molecules. But in our study we have observed the induction of self-structure in poly-A by CHL though the alkaloid binds noncooperatively (as evidenced from Scatchard analysis) to the polynucleotide.

Thermodynamics of the interaction

Thermodynamic parameters for the interaction of CHL with poly-A were evaluated from the temperature dependence of binding constants using UV-Vis absorption spectroscopic studies. Spectrophotometric titrations were carried out at four temperatures namely 15, 20, 25 and 35 °C respectively in CPB buffer. Data are presented in Table 2. The binding constant obtained from analysis of Scatchard plot was found to decrease with increase in temperature while the number of nucleotide occluded sites (n) changed marginally (Table 2). The van't Hoff plot for binding is shown in Fig. 8. Linear van't Hoff plot indicates a very small value of heat capacity change ($\Delta C_P \approx 0$). The values of the thermodynamic parameters are presented in Table 2. The binding was characterized by both negative

enthalpy and entropy changes. This indicates that binding of CHL to poly-A is predominantly enthalpy driven.

The thermodynamic parameters for binding process are contributed from three major components: [i] contributions from hydrogen bonding and hydrophobic part due to interactions between the bound ligand and nucleic acid binding site; [ii] contribution from the conformational changes upon binding in either the nucleic acid or the ligand or both and [iii] contributions from coupled processes like proton transfer, ion release or changes in the water of hydration. Our data revealed that the binding process was favoured by negative enthalpy change and was opposed by negative entropy change. The possible contribution of negative enthalpy change for the binding process of CHL to poly-A may be attributed to the van der Waal's stacking interactions, hydrophobic as well as weak electrostatic interactions. Negative entropy change can be rationalized due to the formation of ordered self structure and the intercalation of CHL which causes loss of translational and rotational degrees of freedom. Such type of behaviour has also been reported for the interaction of another similar bezophenanthridine analogue sanguinarine with poly-A.[21]

Conclusion

In summary, in this study we have reported very high binding affinity of a naturally occurring benzophenanthridine alkaloid CHL to poly-A. From the various spectroscopic studies we have shown that CHL could induce self structure in poly-A. Binding constant was found to be very high and it was of the order of 10^7 M^{-1}. Viscometric data along fluorescence quenching results revealed that the mode of binding of CHL to poly-A was intercalation which leads to self structure induction in the polymer. From sensitized fluorescence experiment it is suggested that there was energy transfer from RNA bases to CHL which in turn corroborated intercalative mode of binding of CHL to poly-A.

Thermodynamic parameters for the binding process revealed both negative enthalpy and entropy changes. Since the interaction of different polymorphic forms of RNA with naturally occurring small molecules is an active area of research in medicinal chemistry and chemical biology, this study renders the scope of exploring the benzophenanthridine group of alkaloids as antiviral drugs.

Acknowledgement

ABP and LH thank to the University Grant Commission, Government of India, for the award of Junior research Fellowship. SB thanks to the University Grant Commission, Government of India, for the award of RGNF research Fellowship.

References

1. P. Nelson, M. Kiriakidou, A. Sharma, E. Maniataki and Z. Mourelatos, *Trends Biochem. Sci.*, 2003, **28**, 534-540.
2. C. C. Esau and B. P. Monia, *Adv. Drug. Deliv. Rev*., 2007, **59,** 101–114.
3. J. Gallego and G. Varani, *Acc. Chem. Res.*, 2001, **34,** 836–843.
4. N. Foloppe, N. Matassova and F. Aboul-ela, *Drug. Discov. Today,* 2006, **11,** 1019-1027.
5. Z. Liu, A. Sall and D. Yang, *Int. J. Mol. Sci*., 2008, **9,** 978–999.
6. S. Fulle and H. Gohlke, *J. Mol. Recog.,* 2010, **23,** 220–231.
7. M. Wickens, P. Anderson and R. J. Jackson, *Curr. Opin. Genet. Dev*., 1997, **7,** 220–232.
8. K. Dower, N. Kuperwasser, H. Merrikh and M. Rosbash, *RNA*, 2004, **10,** 1888–1899.
9. D. Munroe and A. Jacobson, *Mol. Cell. Biol*., 1990, **10,** 3441–3455.
10. M. I. Zarudnaya, D. M. Hovorun, *IUBMB Life,* 1999, **48,** 581–584.
11. B. Tian, J. Hu, H. Zhang and C. S. Lutz, *Nucleic Acids Res.,* 2005, **33,** 201–212.
12. S. L. Topalian, S. Kaneko, M. I. Gonzales, G. L. Bond, Y. Ward and J. L. Manley, *Mol. Cell. Biol.,* 2001, **21,** 5614–5623.
13. S. L. Topalian, M. I. Gonzales, Y. Ward, X. Wang and R. F. Wang, *Cancer Res.,* 2002, **62,** 5505–5509.
14. A. B. Pradhan, L. Haque, S. Roy and S. Das, *PLoS ONE*, 2014, **9,** e87992 1-10.
15. A. Rich, D. R. Davies, F. H. C. Crick and J. D. Watson, *J. Mol. Biol.*, 1961, **3,** 71–86.

16. W. M. Scovell, *Biopolymers*, 1978, **17,** 969–984.

17. A. G. Petrovic and P. L. Polavarapu, *J. Phys. Chem. B.*, 2005, **109,** 23698–23705.

18. F. Xing, G. Song, J. Ren, J. B. Chaires and X. Qu, *FEBS Lett.,* 2005, **579,** 5035–5039.

19. R. C. Yadav, G. S. Kumar, K. Bhadra, P. Giri, R. Sinha, S. Pal and M. Maiti, *Biorg. Med. Chem.,* 2005, **13**, 165–174.

20. P. Giri, M. Hossain and G. S. Kumar, *Int. J. Biol. Macromol.*, 2006, **39,** 210–221.

21. P. Giri and G. S. Kumar, *Biochim. Biophys. Acta.,* 2007, **1770 ,** 1419–1426.

22. O. P. Cetinkol and N. V. Hud, *Nucleic Acids Res.,* 2009, **37,** 611–621.

23. A. Y. Khan, B. Saha and G. S. Kumar, *J. Photochem. Photobiol. B*, 2014, **132**, 17-26.

24. P. Pal and G. S. Kumar, *RSC Adv.,* 2014, **4**, 25666-25674.

25. D. Gibson, *Pharmacogenomics J*., 2002, **2,** 275–276.

26. M. Maiti and G. S. Kumar, *Med. Res. Rev.,* 2007, **27,** 649-695.

27. N. Ahmad, S. Gupta, M. M. Husain, K. M. Heiskanen and H. Mukhtar, *Clin. Cancer Res.,* 2000, **6,** 1524-1528.

28. S. Yamamoto, K. Seta, C. Morisco, S. F. Vatner and J. Sadoshima, *J. Mol. Cel. Cardiol.,* 2001, **33,** 1829-1848.

29. J. O'Neill, M. Manion, P. Schwartz and D. M. Hockenbery, *Biochim. Biophys. Acta,* 2004, **1705,** 43-51.

30. V. M. Adhami, M. H. Aziz, S. R. Reagan-Shaw, M. Nihal, H. Mukhtar and N. Ahmad, *Mol. Cancer. Ther.*, 2004, **3,** 933-940.

31. A. Cabrespine, J. O. Bay, C. Barthomeuf, H. Cure, P. Chollet and E. Debiton, *Anticancer Drugs,* 2005, **16,** 417-422.

32. K. M. Ansari, A. Dhawan, S. K. Khanna and M. Das, *Cancer Lett.,* 2006, **244,** 109–118.

33. L. P. Bai, Z. Z. Zhao, Z. Cai and Z. H. Jiang, *Bioorg. Med. Chem.,* 2006, **14,** 5439-5445.

34. Z. F. Zhang, Y. Guo, J. B. Zhang and X. H. Wei, *Arch. Pharm. Res.,* 2011, **34,** 791-800.

35. M. Maiti and G. S. Kumar, *J. Nucl. Acids*, 2009, **2010**, 1–24.

36. M. Maiti, S. Das, A. Sen, A. Das, G. S. Kumar and R. Nandi, *J. Biomol. Struct. Dyn.,* 2002, **20,** 1-10.

37. S. Das, G. S. Kumar and M. Maiti, *Biophys. Chem.,* 1999, **76,** 199–218.

38. P. Giri and G. S. Kumar, *J. Photochem. Photobiol A,* 2008, **194,** 111–121.

39. S. J. Chmura, M. E. Dolan, A. Cha, H. J. Mauceri, D. W. Kufe and R. R. Weichselbaum, *Clin. Cancer Res.,* 2012, **6,** 737-742.

40. T. Funakoshi, T. Aki, H. Nakayama, Y. Watanuki, S. Imori and K. Uemura, *Toxicol. In Vitro*, 2011, **25,** 1581-1587.

41. J. Hammerova, S. Uldrijan, E. Taborska and I. Slaninova, *J. Dermatol. Sci.*, 2011, **62,** 22-35.

42. S. K. Lee, W. G. Qing, W. Mar, L. Luyengi, R. G. Mehta and K. Kawanishi, *J. Biol. Chem.,* 1998, **273,** 19829-19833.

43. R. Yu, S. Mandlekar, T. H. Tan and A. N. T. Kong, *J. Biol. Chem.,* 2000, **275,** 9612-9619.

44. P. Basu, D. Bhowmik and G. S. Kumar, *J. Photochem. Photobiol. B,* 2013, **129,** 57-68.

45. J. Li, B. Li, Y. Wua, S. Shuang, C. Dong and M. M. F. Choi, *Spectrochim. Acta. Part A,* 2012, **95,** 80–85.

46. J. B. Chaires, N. Duttagupta and D. M. Crothers, *Biochemistry*, 1982, **21**, 3933-3940.

47. G. Scatchard, *Ann. N Y Acad Sci.,* 1949, **51,** 660–662.

48. J. D. McGhee and P. H. von Hippel, *J. Mol. Biol.,* 1974, **86,** 469–489.

49. P. Job, *Annal. di Chimica Applicata,* 1928, **9,** 113-203.

50. D. Bose, D. Ghosh, P. Das, A. Girigoswami, D. Sarkar and N. Chattopadhyay, *Chem. Phys. Lipids,* 2010, **163,** 94–101.

51. J. R. Lakowicz, Principles of Fluorescence Spectroscopy; Plenum Press: New York, U.S.A., 2006.

52. S. Das and G. S. Kumar, *J. Mol. Struct.,* 2008, **872,** 56–63.

53. C. V. Kumar, E. H. A. Punzalan and W. B. Tan, *Tetrahedron,* 2000, **56,** 7027-7040.

54. J. B. LePecq and C. Paoletti, *J. Mol. Biol.*, 1967, **27,** 87–106.

55. N. C. Garbett, N. B. Hammond and D. E. Graves, *Biophys. J.,* 2004, **87,** 3974–3981.

56. G. Zhang, J. Guo, J. Pan, X. Chen and J. Wang, *J. Mol. Struct.***,** 2009, **923,** 114-119.

57. P. Giri and G. S. Kumar, *Archives Biochem. and Biophys,* 2008, **474,** 183-192.

58. P. Das, A. Chakrabarty, B. Haldar, A. Mallick and N. Chattopadhyay, *J. Phys. Chem*. *B*, 2007, **111,** 7401-7408.

59. L. S. Lerman, *J. Mol. Biol.,* 1961, **3,** 18-30.

60. H. M. Berman and P. R. Young, *Ann. Rev. Biophys. Bioeng.*, 1981, **10,** 87-114.

61. D. Chuan, W. Yu-xia and W. U. Yan-li, *Photochem. Photobiol. A*, 2005, **174,** 15-22.

62. C. V. Kumar and E. H. Asuncion, *J. Am. Chem. Soc.*, 1993, **115**, 8547-8553.

63. B. B. Johnson, K. S. Dahl, I. Tinoco Jr, V. I. Ivanov and V. B. Zhurkin, *Biochemistry,* 1981, **20,** 73-78.

64. M. Polak and N. V. Hud, *Nucleic Acids Res.*, 2002, **30,** 983–992.

65. S. Das, S. Parveen and A. B. Pradhan, *Spectrochim. Acta Part A,* 2014, **118,** 356–366.

Figure legend

Fig. 1. Chemical structure of CHL.

Fig. 2. Representative absorption and fluorescence emission spectral changes of CHL in presence of poly-A in CPB buffer at 25 °C. (A) curves 1-8 denote the absorption spectrum of CHL (5.06 μM) treated with 0, 1.8, 3.3, 4.9, 6.6, 8.4, 10.1 and 13.6 μM of poly-A respectively. (B) curves 1-9 denote the fluorescence spectrum of CHL (3.38 μM) treated with 0, 0.88, 1.95, 3.21, 4.77, 6.75, 8.94, 10.55 and 12.50 μM of poly-A respectively. The excitation wavelength was 400 nm at a spectral excitation and emission bandwidth of 5 and 5 nm, respectively.

Fig. 3. Scatchard plots of the binding of CHL with poly-A monitored from (A) absorption spectrophotometry and (B) spectrofluorimetry. The points in the figures represent the data points and the solid line represents the best fit to the McGhee–von Hippel equation [1]. The experimental points are the average of four determinations.

Fig. 4. A plot of change of relative specific viscosity of poly-A with increasing concentration of CHL in CPB buffer at 25 °C. The concentrations of poly-A was 500 μM.

Fig. 5. (A) Fluorescence excitation spectrum of CHL recorded in presence of poly-A at emission of wavelength 564 nm. (B) Sensitized fluorescence spectra of CHL in presence (curve 1) and in absence of poly-A. (C) Variation of relative quantum efficiency of CHL in the presence of poly-A. (D) Energy transfer scheme illustrating the sensitization of alkaloid emission by the RNA bases. All the spectra were taken in CPB buffer at 25 °C.

Fig. 6. Circular dichroism spectra of poly-A (50.0 μM) with varying concentrations of CHL in CPB buffer at 25 °C. The curves 1–8 represent the CHL concentrations of 0, 3.4, 6.8, 10.1, 13.5, 15.1, 16.8 and 18.5 μM respectively.

Fig. 7. (A): CD spectra of poly-A (50.0 μM) in absence (red) and in presence of (blue) 15.1 μM CHL in CPB buffer at 25 °C. (B): CD melting profile of free poly-A (50.0 μM) in

CPB buffer. (C) CD melting profile of a solution containing poly-A (50.0 μM) in presence of 15.1 μM CHL in CPB buffer.

Fig. 8. van't Hoff plot for the complexation of CHL with poly-A in CPB buffer.

Fig. S1. Absorption (Panel A) and fluorescence excitation (Panel B) spectra of iminium (curve 1) and alkanolamine (curve 2) form of CHL (2.56 μM) at 25 °C. Spectrum of iminium form was taken in CPB buffer (pH 6.5) and spectrum of alkanolamine form was taken in 10 mM carbonate-bicarbonate buffer containing 25 mM NaCl (pH 10.1). Excitation and emission bandwidth were 5 and 5 nm, respectively.

Fig. S2. Job's plot for the binding of CHL poly-A in CPB buffer at 25 °C. The relative difference in fluorescence intensity at 564 nm was plotted against the mole fraction of CHL added.

Fig. S3. Variation of the anisotropy of CHL fluorescence as a function of concentration of poly-A. λ_{ex} and λ_{em} for CHL was 400 and 564 nm respectively.

Fig. S4. Stern-Volmer plots for the quenching of CHL fluorescence by KI in the absence (●) and in presence (●) of poly-A in CPB buffer at 25 °C.

Fig. S5. Fluorescence excitation spectra of free CHL (2.56 μM, curve 1) and poly-A (25.6 μM, curve 2) in CPB buffer at 25 °C. Excitation and emission bandwidth were fixed at 5 and 5 nm respectively.

Table 1

Binding parameters for the interaction of CHL with poly-A in CPB buffer at 25 °C obtained from spectrophotometry and spectrofluorimetry.[a]

Parameters	Methods	Values
K′ x10^{-7}, the intrinsic binding constant (M^{-1})	[A] Spectrophotometry	2.06±0.10
	[B] Spectrofluorimetry	2.14±0.07
n, the no of base occluded	[A] Spectrophotometry	1.80±0.05
	[B] Spectrofluorimetry	2.32±0.04
K_{SV}, the Stern Volmer quenching constant (L mol^{-1})	Spectrofluorimetry	[i] Free: 12.1±1.30
		[ii] Bound: 8.5±0.70
Fluorescence polarization anisotropy	Spectrofluorimetry	[i] Free:0.040±0.002
		[ii] Bound:0.13±0.01

[a]Average of three determinations

Table 2

Binding and thermodynamic parameters for the interaction of CHL with poly-A in CPB buffer obtained from absorption spectrophotometry.[a]

Temperature (ºC)	K′ x10^{-7}(M^{-1})	n	$\Delta G°$ (kJ mol^{-1}) at 25 ºC	$\Delta H°$ (kJ mol^{-1})	$T\Delta S°$ (kJ mol^{-1}) at 25 ºC
15	4.49±0.20	1.75±0.10	-41.75±2.0	-50.66±2.5	-8.91±0.50
20	3.05±0.15	1.79±0.15			
25	2.06±0.10	1.80±0.20			
35	1.14±0.08	1.90±0.30			

[a]Average of three determinations

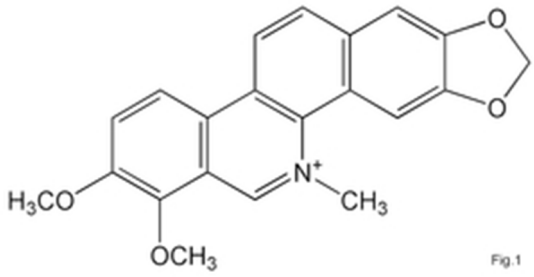

Fig.1

25x12mm (300 x 300 DPI)

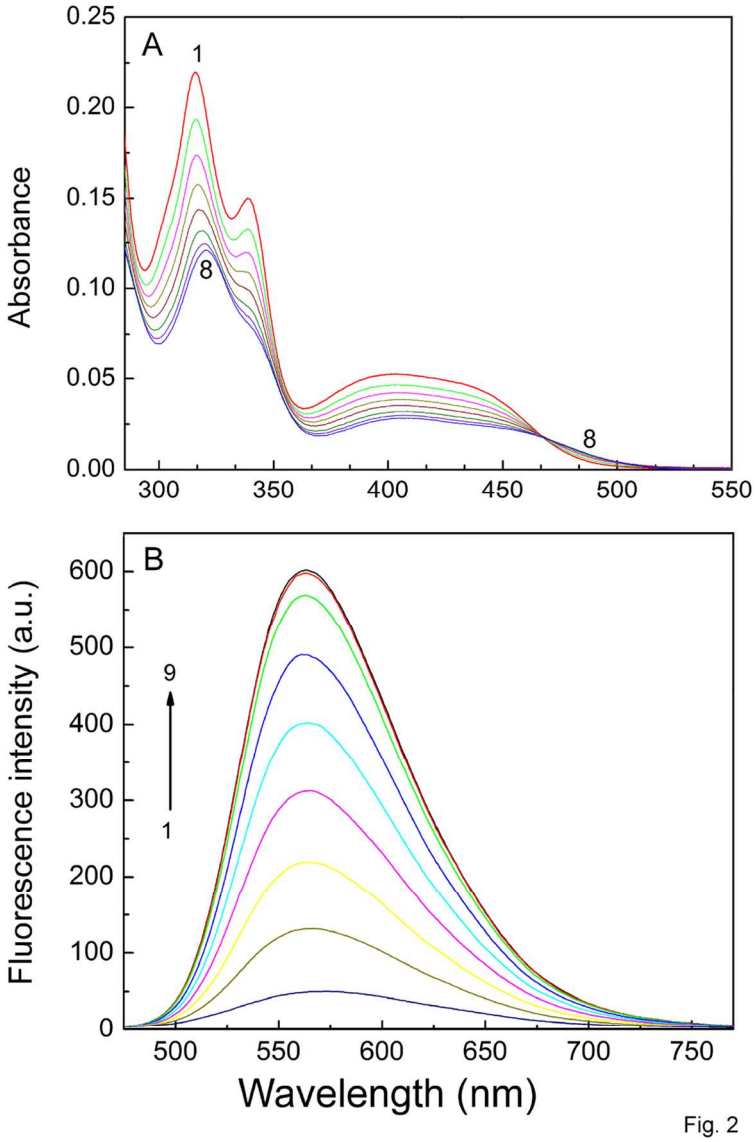

Fig. 2

106x160mm (300 x 300 DPI)

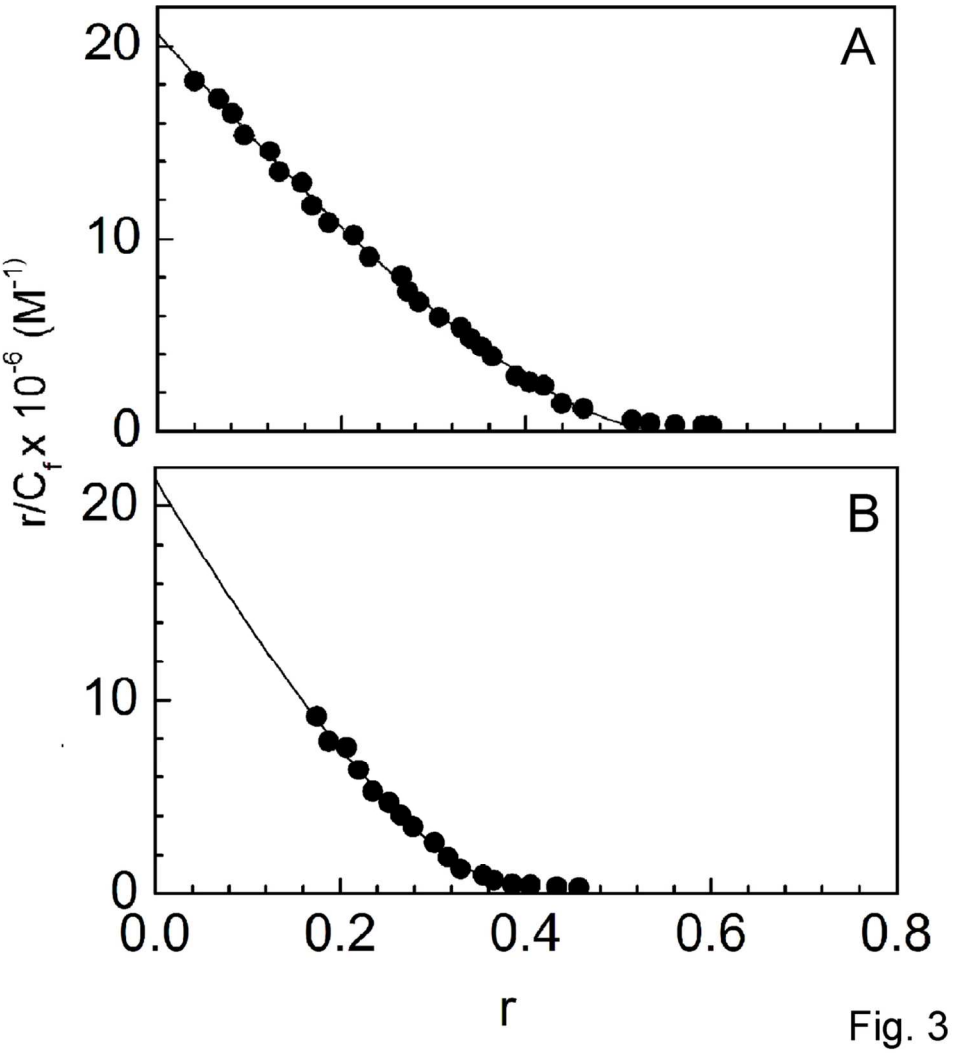

Fig. 3

113x126mm (300 x 300 DPI)

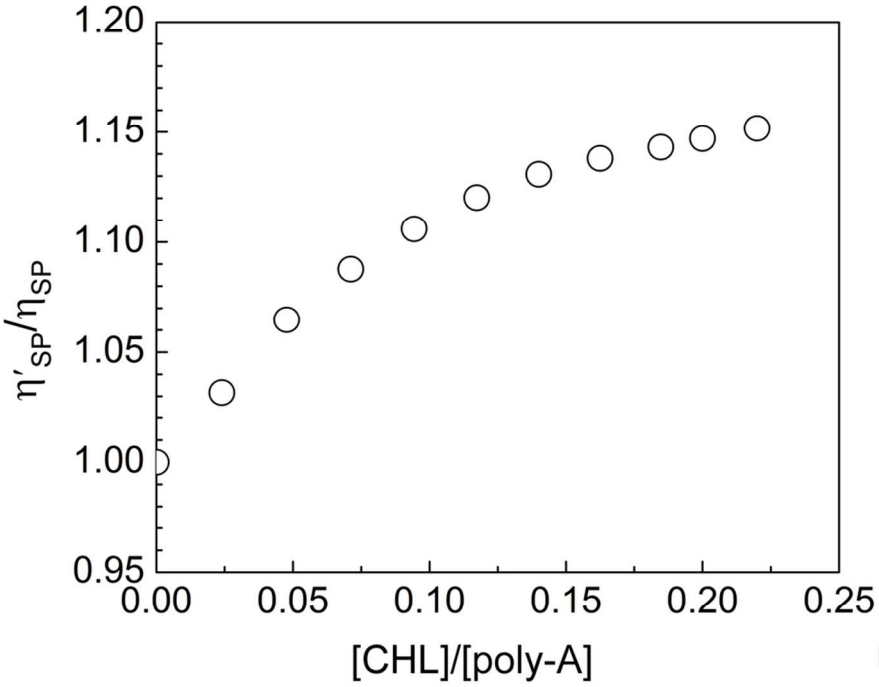

Fig. 4

97x74mm (300 x 300 DPI)

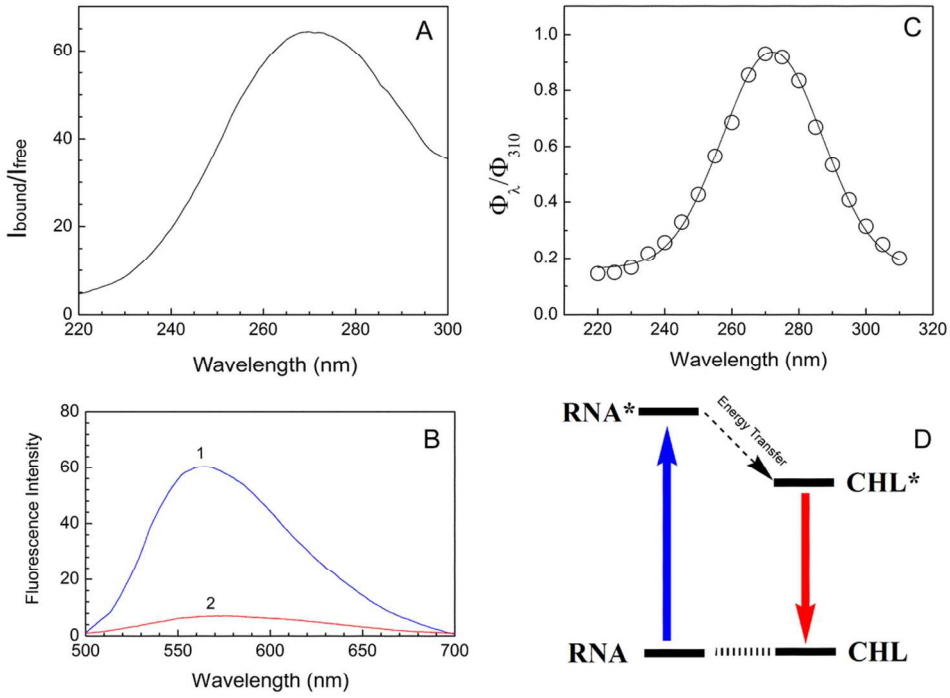

Fig. 5

104x86mm (300 x 300 DPI)

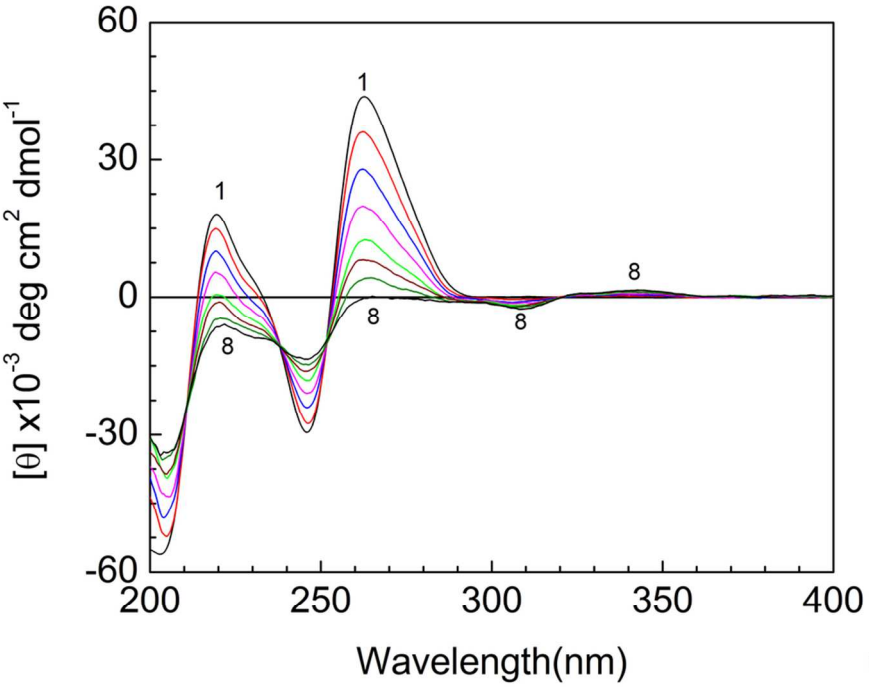

Fig. 6

97x74mm (300 x 300 DPI)

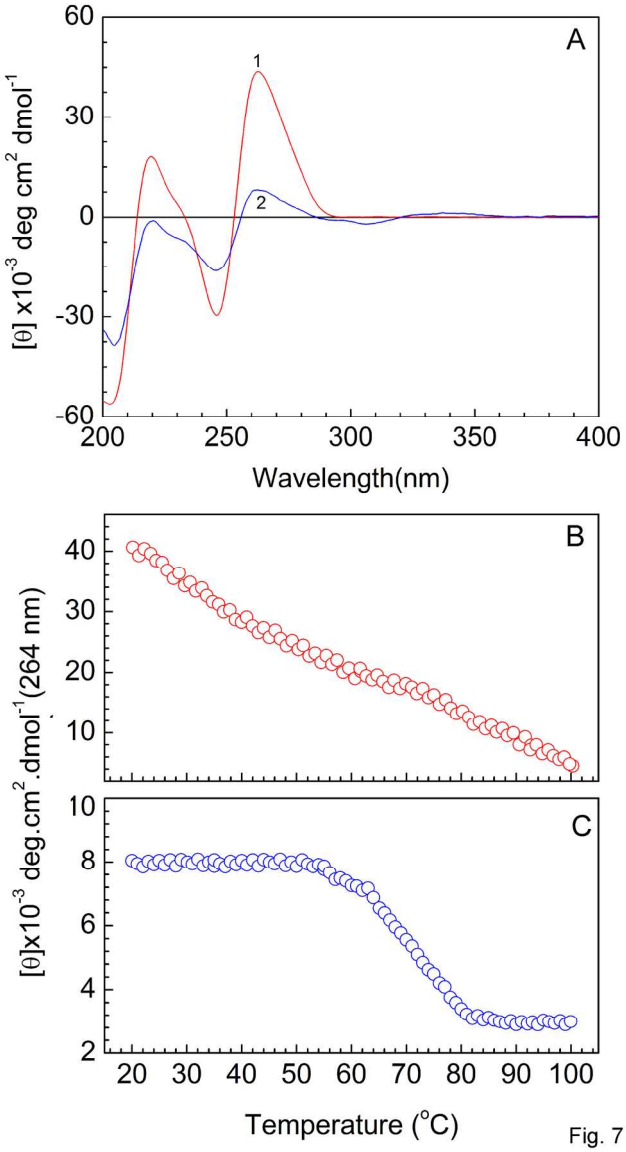

Fig. 7

127x226mm (300 x 300 DPI)

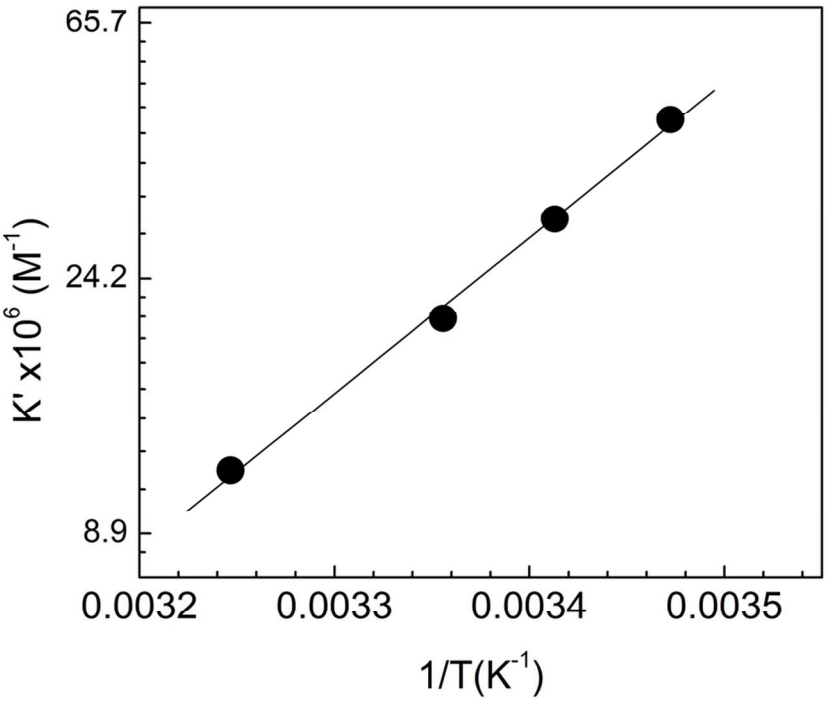

Fig. 8

101x80mm (300 x 300 DPI)